Semi-Active Hybrid Topology with Three-level DC-DC Converter for Electric Vehicle Application

Felipe Machado, Carlos Henggeler Antunes
R&D Institute INESC Coimbra
Depart. Electrical and Computer Engineering
University of Coimbra
Polo II, 3030 Coimbra, Portugal
machado.felipe88@gmail.com; ch@deec.uc.pt

Maxime R. Dubois, João P. Trovão*
e-TESC Laboratory / *R&D Unit INESC Coimbra
Department of Electrical & Computer Engineering
University of Sherbrooke
Sherbrooke, QC, J1K 2R1, Canada
{Joao.Trovao, Maxime.Dubois}@USherbrooke.ca

***Abstract*—A bidirectional DC-DC converter is employed to control the power of the secondary storage element according to the references set by the energy management system in a semi-active hybrid topology for an urban electric vehicle. This study proposes an improved DC-DC converter to connect supercapacitors to the main DC bus. The DC-DC converter controller is oriented by references provided by an online management algorithm. The feeding system model including its inner control layer is addressed to introduce the energy strategy system, considering an improved three-level DC-DC converter. Decisions at the energy management strategy level are supported by a fast meta-heuristic approach. Simulations using Matlab-Simulink™ are provided to demonstrate the performance of the selected topology in order to keep the batteries and supercapacitors within physical limits on the driving cycle.**

***Keywords*—Electric Vehicles, Three-level DC-DC Converter, Linear control, Energy Management Strategy, Batteries, Supercapacitors.**

I. Introduction

Electro-mobility introduces new challenges for vehicle manufacturers; the number of mechanical components is reduced but the Electric Vehicle (EV) overall complexity is increased. Research is underway on new feeding topologies to reach higher range, climbing and acceleration capability, and energy efficiency.

Therefore, hybrid topologies of energy storage systems, including batteries and supercapacitors (SCs), should be appropriately combined aimed at improving performance [1]. SCs-assisted EVs are an attractive alternative to battery-only EVs with high specific power batteries. The objective is to combine characteristics of high specific energy (e.g. energy battery cells) and high specific power (e.g. SCs) storage elements in feeding unified power supply system. Different topologies, in which SCs are either actively, semi-actively or passively controlled have been proposed with increasing complexity and performance [2]-[4]. The automotive industry has paid an increasing attention to the semi-active topology, presented in Fig. 1, which couples batteries and SCs while using only one DC/DC converter [5]. In this topology, a battery pack is directly connected to the DC bus and serves essentially as an energy buffer. The SCs pack is linked to the DC bus by the DC-DC converter.

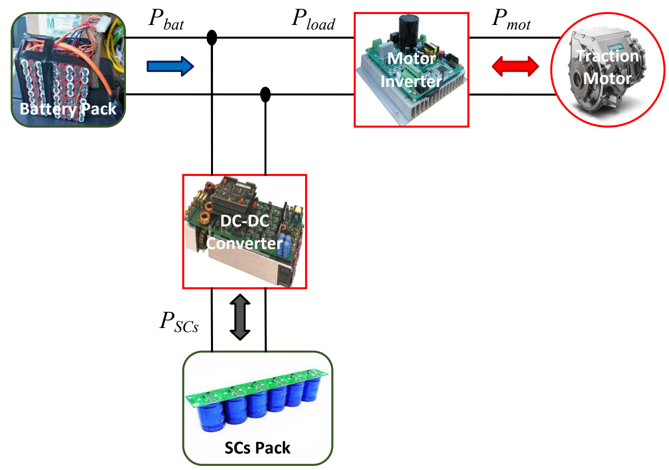

Fig. 1. Powertrain architecture with semi-active topology.

SCs provide the advantage of supplying higher power peaks for short time, which can be used for the vehicle accelerations. The result is higher vehicle dynamics and lower losses during the power peaks. The conventional approach for such improved dynamic is accomplished by manipulating the SCs DC-DC converter to control the DC bus voltage with a more regulated inverter voltage. As the bidirectional DC-DC converter is the only controllable unit in the supply system, its selection is of critical importance since it greatly affects the overall system efficiency and it should adjust the characteristics of the SCs to the powertrain architecture.

Past studies have proposed and evaluated various types of bidirectional DC-DC converters for EVs applications, including efficiency comparisons, assessed for particular power levels with fixed input/output parameters [6]-[10]. However, an effective efficiency evaluation of converters for EVs should include the power variations, voltage and current ranges of both batteries and SCs while driving the road cycle. Recently, some studies proposed using three-level converters [11]-[13] as bidirectional DC-DC converters to improved EV performance. Using the conclusions of these research works, this paper introduces the three-level converter in combination with the design and implementation of an advanced Energy Management System (EMS) to improve the efficiency of the overall power architecture of a specific EV. An EV using batteries and SCs is studied. Their functional models are developed and an inner control layer is proposed as lower level of an EMS design. The management algorithm appears on the first control layer in order to take into consideration the system dynamics and the State of the Charge (SoC) of the storage elements, addressing the two fundamentals problems of the vehicle management: energy (Long-term planning) and power (Short-term planning) issues, using a fast meta-heuristic optimization technique [14]. The proposed approach considers the diverse specifications of the system using a set of constraints. An online algorithm is proposed with a real-time processor without a priori knowledge of the driving cycle profile.

This paper is organized as follows. In Section II, a description of the powertrain system is given. The model and the development of the inner control layer of the three-level DC-DC converter is presented in Section III. The energy management algorithm based on a hybrid meta-heuristic approach is presented in Section IV. The main results of the e-VUE prototype on a standard driving cycle are given in Section V. Finally, some conclusions area drawn in Section VI.

II. Electric Vehicle Prototype Description

The original version of the EV prototype under study is powered using a Li-ion battery pack (7.68 kWh) and propelled by a rear-mounted Permanent Magnet Synchronous Motor (PMSM) of 30 kW, 5500 rpm. The prototype is based on a second generation of a SMART vehicle as results of a full-electric propulsion vehicle conversion made by ATEUS (*Association des Transports Électriques de l'Université de Sherbrooke*) under the e-VUE project and shown in Fig. 2. Table I presents the vehicle main characteristics. The performance of the e-VUE prototype will be evaluated to derive an improved semi-active topology to couple a SCs pack using a three-level DC-DC converter. The proposed powertrain scheme is the same as in Fig. 1, with a three-level DC-DC converter. The battery pack is directly connected to the DC bus motor drive while the SCs pack is connected to this DC bus using a three-level converter [11].

The bidirectional DC-DC converter is used to control the current flow of the SCs to or from the DC bus motor drive. Some challenges are related to the selection of the suitable components for the implementation of the three-level converter. At this moment, a first simulation phase is under evaluation for the full-scale prototype study.

Fig. 2. ATEUS electric vehicle prototype

TABLE I. Electric Vehicle Specifications

Variable	Symbol	Value	Units
Vehicle mass (without battery and SCs packs)	m	795	kg
Rolling resistance force	μ_{rr}	0.02	-
Gravity acceleration	g	9.81	m/s^2
Air density @ 20ºC	ρ	1.223	kg.m^{-3}
Aerodynamic drag coefficient (with driver)	C_D	0.35	-
Vehicle front area	A_f	2.4	m^2
Wheels radius	r	0.38	m
Gearbox transmission ratio	G_{gb}	3 (3:1)	-
Gearbox transmission efficiency	η_{gb}	92	%

As in this configuration, the battery pack is directly coupled to the DC bus motor drive, the voltage variation is directly linked to the battery current discharge. Thus, the SCs and its DC-DC converter should stabilize the DC bus voltage at the motor drive terminals, through the injection or storage of current to the SCs pack.

The original supply system is based on a battery pack composed by $LiFePO_4$ cells, 3.2 V and 14.5 A@1C. To implement the SCs pack, the use of 250 F modules (16.2 V) is considered to reduce the current stress of the batteries and fundamentally improve the EV dynamics. The characteristics of the energy storage elements used to perform this study are presented in Table II.

TABLE II. Characteristics of the Energy Storage System

Variable	Symbol	Value	Units
Battery (3.2 V EiG LiFePO4 cell)			
Battery pack Power	P_{Bat}	[- 1.2, 9.5]	kW
Battery pack SoC Limits	SoC_{Bat}	[0.2, 1]	-
Min. cell open-circuit voltage	$V_{Bat}^{OC\_min}$	2.4	V
Cell no-load voltage drop	δ_{bat}	1.0	V
Max. cell open-circuit voltage	$V_{bat}^{OC\_max}$	3.4	V
Cell internal resistance	R_{cell}	5	mΩ
Number of batteries in series	N_{cell}	96	-
Num. of battery's bank in parallel	n_{cell}	2	-
Battery mass	M_{cell}	0.4	kg
Supercapacitors (MAXWELL BMOD0250 modules)			
SC module Capacitance	Cap_{SCs}	250	F
SC pack Power	P_{SCs}	[- 96, 96]	kW
SC pack SoC Limits	SoC_{SCs}	[0.5, 1]	-
Min. SC open-circuit voltage	$V_{SCs}^{OC\_min}$	0	V
SC no-load voltage drop	δ_{SCs}	16.2	V
SC pack operation range	V_{SCs}^{OC}	[64.8, 129.6]	V
SCs module internal resistance	R_{SCs}	4.1	mΩ
Number of SC's module in series	N_{SCs}	8	-
Num. of SC's module in parallel	n_{SCs}	2	-
SC Mass	M_{SCs}	4.45	kg

III. DC-DC Converter Topology

Projects involving DC-DC boost converters are generally based on two-level single-phase converters. Changes in this topology are mostly focused on interleaved techniques [11] that only solve the problem of high current and do not optimize the size of inductors and capacitors, the heavier and more expensive devices in a high power DC-DC converter.

To reduce the size of those passive components the best option has been to use the highest switching frequency that the switching devices (e.g. IGBTs) could handle. However, if we can divide the step-up voltage in a three-level converter instead of the common two, then we can obtain results that effectively match with doubling the frequency of the switching devices. This also brings advantages to voltage ratings of the switching devices and capacitors. Such solutions are also adopted in systems with similar requirements [11].

A. Three-level converter

A multi-level converter is a solution used for high voltage applications. The DC bus voltage is divided across multiple steps, which allows for lower-voltage devices, reducing costs and size compared to normal boost converters [11]. In the three-level converters, the switches and capacitors divide the main DC bus voltage in two, as presented in Fig. 3. The inductor is the same for these two-steps, but the frequency is double the frequency of the PWM modules. A full description of this topology was presented in [11].

As presented in Fig. 3, the implemented three-level DC-DC converter is composed by four IGBTs (SW_1A, SW_1B, SW_2A and SW_2B), an inductor $L2$ and two filter capacitors C1 and C2. These capacitors are series connected and the goal is to maintain an equal voltage in both of them. PWM frequencies are the same, but with a phase shifting of π rad between PWM 1 and PWM 2. Duty cycles values $d1$ and $d2$ are approximately equal, and a small deviation between them balances the V_{C1} and V_{C2} voltages. Assuming $d1 = d2 = d$, we can compute the V_{bus} as a function of the duty cycle, d, and the input voltage, V_{SC}, as:

$$V_{SC} = d \cdot V_{bus} \quad (1)$$

The current ripple over the inductance $L2$ can be computed as a function of the duty cycle. Regarding the EV dynamics and the voltage and current variations in SCs, the duty cycle will be adjustable to reach the management objectives. Thus with a stipulated maximum current ripple ($\Delta I_{L2_{\text{MAX}}}$), typically under 5%, the value of the inductance can be found using (2):

$$L_2 \geq \frac{V_{bus_{\text{MAX}}}}{\Delta I_{L2_{\text{MAX}}} \cdot f_{SW} \cdot 16} \quad (2)$$

where f_{SW} is the switching frequency of the converter.

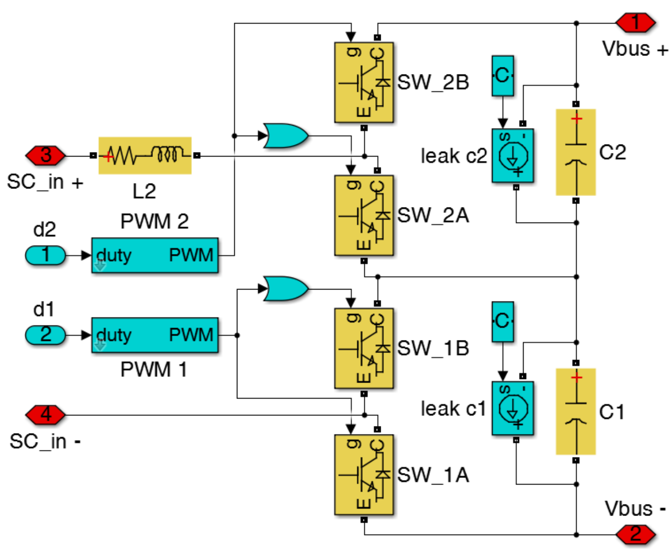

Fig. 3. Simulation model of the three-level converter.

Regarding the capacitors design, these are essentially used to reduce the input voltage ripple. For this purpose, some design restriction should be guaranteed as capacitors' peak and RMS current.

Concerning the voltage ripple criteria, we assume that the capacitance of the filter capacitors is equal: $C1 = C2 = C$. In fact, the voltage ripple depends on two ranges of the duty cycles, namely for $d < 0.5$ and $d \geq 0.5$. As the purpose of this converter is to be used with a SCs rated for less than half of the minimum batteries voltage, the minimum capacitance of the filters can be computes as in (3):

$$C \geq \frac{P_{out}(1 - d_{\text{MIN}})}{v_{bus} \cdot \Delta v_{bus_{\text{MAX}}} \cdot 2 \cdot f_{SW}} \quad (3)$$

where P_{out} is the output power of the converter and $\Delta v_{bus_{\text{MAX}}}$ is the maximum value of the input voltage ripple.

By comparing this topology with a single-phase two-level topology (Fig. 4), maintaining the same frequency and ripple requisites, we were able to reduce the inductance in one-fourth of the size and the filter capacitor in one-third.

To simulate the additional complexity of control in a three-level converter versus a common two-level, the tolerance values of the capacitors C1 and C2 have to be considered. In this model, differences in capacitance, series resistance and also leaked current are included. Moreover, the model naturally unbalances the voltage in each capacitor, leaving the task of balancing the voltages for the control layer.

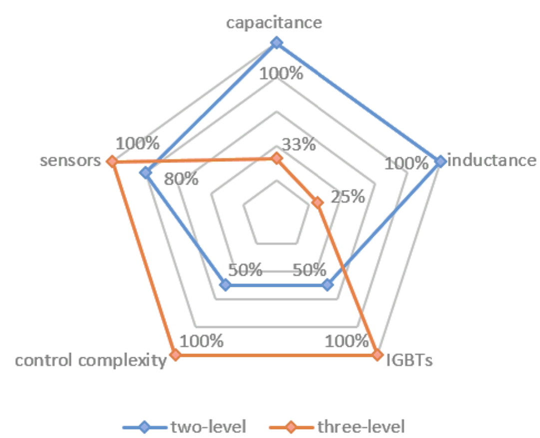

Fig. 4. Comparison bettwen converter topologies

B. Control definition

At first glance, the control of the duty cycles is very similar to other PI based current controllers for boost converters. The definition of the control law should consider the reference decision of the power requested to the battery P_{bat}^{ref} given by the EMS presented below.

In Fig. 5, the implemented control layer is presented. The control law is based on two separated controllers, one is the PI current controller that receives a decoupled current reference signal from the EMS and the other is a PI controller that assures the balance between V_{C1} and V_{C2}.

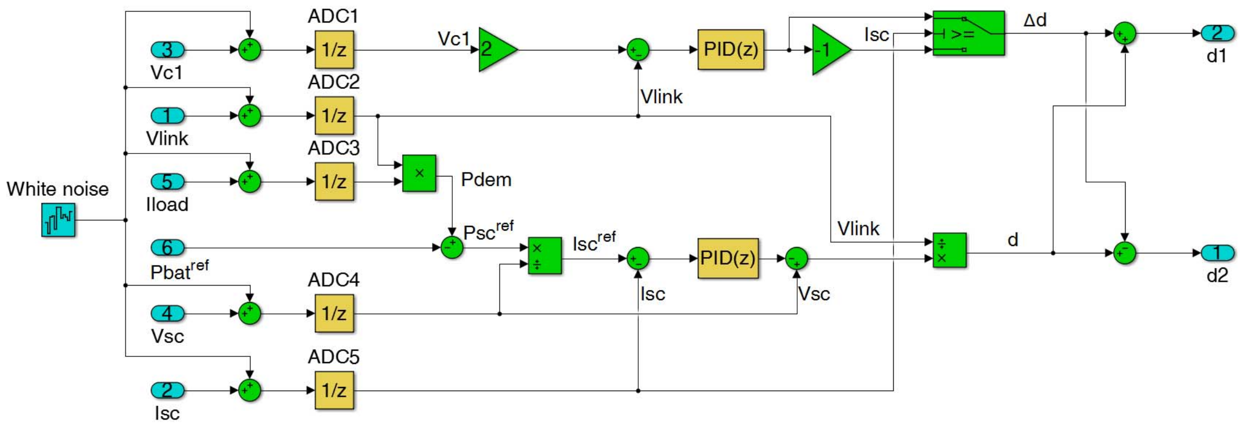

Fig. 5. Control layer implemented for the three-level converter

As the controller should output a very close $d1$ and $d2$ signals, the current controller output mainly sets the duty cycle values. The small difference between $d1$ and $d2$ (Δd) is the output of the balancing controller. The Δd signal is the same as the direction of the current I_{SC}.

To be able to simulate the controller closer to the reality, white noise is included in all the sensors signals and everything is considered in discrete time with the same rate as a microprocessor would handle.

As the EMS is updated in a smaller time base than the controller, P_{bat}^{ref} should hold until a different value results from the EMS, while the SCs follow all the load changes. Based on the total power demanded by the vehicle, P_{dem}, and the storage elements' SoC, the SC power references, P_{SC}^{ref}, is given by:

$$P_{SC}^{ref} = P_{dem} - P_{bat}^{ref} \tag{4}$$

After, the current reference of the SC, I_{SC}^{ref} is computed using:

$$I_{SC}^{ref} = \frac{P_{SC}^{ref}}{V_{SC}} \tag{5}$$

Basically, the proposed approach coordinates a three-level DC-DC converters controller (Control Layer) by the combination a rule-based control strategy oriented by an operation mode dependence (Long-term Planning) using an optimization strategy as decision maker (Short-term Planning). Fig. 6 shows the EMS architecture.

IV. Energy Management Problem

The main objective of an EMS in this type of vehicle is to improve the maximum power of the system without overloading the batteries while keeping the SCs SoC at a certain level. To improve the batteries' lifetime, lower fluctuations of batteries' power are welcome. The SCs SoC needs to be enough to deal with the power fluctuations and absorb all the regenerative braking.

In this work, the energy management problem is solved online without knowledge of the driving cycle and the SCs are recharged using the batteries when required. The formulation of the energy management problem in EVs with multiple sources is fundamentally based on three essential objectives: Long-Term Planning (energy management), responsible for the definition of an overall management strategy; Short-Term Planning (power management), whose main function is to define a plan of action that will produce the reference signals for the controller; and the Control Layer, which has been discussed in the previous section. A diagram of this real-time system is displayed in Fig. 6.

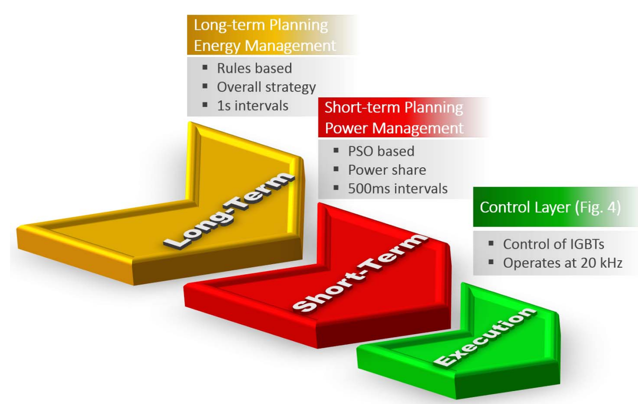

Fig. 6 Division of tasks of the EMS architecture

A. *Long-term Planning*

The global strategy of this layer is to create the bounds for the power requested to SCs and batteries at every step of P_{dem}. The main advantage of using rules to define the strategy is the simplicity of the implementation, requiring very low processing capabilities [15]. The design of these rules takes into account the storage elements' sizing and capacities, then being specific for this EV and previously adjusted using the methodology proposed in [16]. This layer is updated periodically at a rate of 1s, in a "dynamic rule restriction" process.

The set of rules determines the lower bounds LB_j and upper bounds UB_j for every C_j in each source j [16]. To have a more realistic set of rules, P_{dem} is classified according to basic vehicle operation: regenerative braking, standing, cruising or hard acceleration.

For each of these classes, the SCs SoC sets the batteries' bounds in a way to drive the SCs SoC up, down or constant. In order to consider emergency situations such as any of the SoC_j under the minimum thresholds or power demand higher than the system capabilities, higher priority rules can shut-down the system and stop the vehicle. An example of a cruising operation can be seen in Fig. 7 (which is fully explained in [16]).

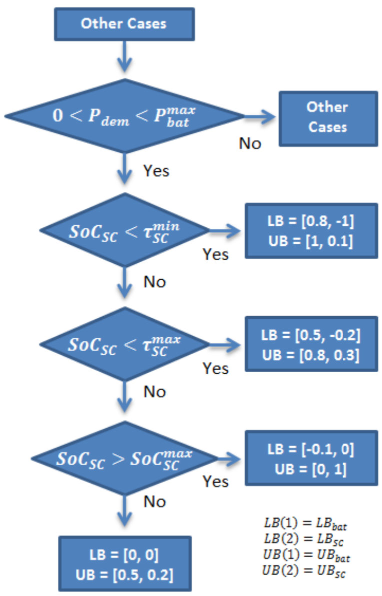

Fig. 7. Rule-based search space restriction for cruising operation

B. *Short-term Planning*

The vehicle's movement has a stochastic component, and it is necessary to consider a power management layer able to respond in real-time to new driving options. This dynamic problem is solved using a meta-heuristic approach able to provide (near) optimal solutions in every instant and exploiting the search space delimited by the Long-term Planning. This approach utilizes Particle Swarm Optimization (PSO) adapted to the problem, thus creating a balance between diversification and intensification mechanisms to obtain (near) optimal solutions with a low computational effort [17].

Considering on-going EV prototype, the mathematical model is proposed in (6) and is developed to find the power fed to or stored by the storage element in each instant $[k]$. $C_{bat}[k]$ and $C_{SC}[k]$ are the variables responsible for defining the power in each storage element, in each instant $[k]$, which are chosen based on the bounds defined in the Long-term Planning. $V_j[k]$ is the voltage measured at element j, at each instant $[k]$.

$$f = \min_{C_{bat},C_{SC}} \left| P_{dem}[k] - \left[C_{bat}[k] \cdot P_{bat}^{max}[k] + C_{SC}[k] \cdot P_{SC}^{max}[k] \right] \right| \quad (6)$$

s. t.:

$$LB_j[k] \leq C_j[k] \leq UB_j[k]$$
$$P_j[k] = C_j[k] \cdot P_j^{max}[k]$$
$$P_j^{max}[k+1] = V_j[k] \cdot I_{j\_Ref}$$
$$P_j^{min}[k] \leq P_j[k] \leq P_j^{max}[k]$$

with $j \in \{bat, SC\}$.

V. Simulation Results

The simulation was held in Matlab/Simulink®. Some considerations where made to approximate this simulation as close as possible to reality, such as: sensor's noise, different leakage currents in capacitors $C1$ and $C2$, and inductor losses. Those differences are crucial to validate the EMS. The driving cycle used for this test was VWU-CITY, using as reference the double of the normalized speed. All the considerations presented in Table I and II were taken into account for the vehicle model.

Analysing Fig. 8, we see that a large part of the higher frequencies of the power demand were transferred for the SCs pack. The SCs SoC always charge up to 90% and even after the higher discharges, never gets below 70%. The great advantage of this system is shown around the 475s mark, where P_{dem} requires almost 30 kW and the batteries maintain at 15 kW while the SCs fulfil the rest.

This displays an adequate behaviour of the EMS, showing that it was always able to determine the adequate response of the batteries without any prior knowledge of the driving cycle.

Relatively to the losses of the switching elements, filter inductor and capacitors, and the three-level converter performance, these preliminary results present a quite optimistic behaviour that should be verified on the overall operation range.

VI. Conclusions

The usability of a three-level converter in a semi-active hybrid topology for a real EV was presented. The simulations results validate the integration of a three-level topology for DC-DC converter implementation with efficiency improvement of the overall power architecture. The paper also presents the specific control layer of this converter topology and its coupling with an EMS based on an online energy sharing optimization approach between the storage elements without prior knowledge of the power demand profile. The proposed management algorithm uses the dynamics of system and the energy levels of the storage elements, addressing energy (Long-term planning) and power (Short-term planning) issues. The stress in the current batteries decrease and the DC bus voltage is positioned in a range where the motor drive does not reduce the efficiency for most operation points.

The proposed approach was validated in a specific case study of a semi-decoupled hybrid topology to combine batteries and SCs in EV application. The proposed approach can be evaluated as an alternative, after a careful cost assessment, taking into account the overall efficiency improvement and the complexity increase associated with the DC-DC converter. The next step in this research will be the development of the prototype of the three-level DC-DC converter and its coupling with the other components of the powertrain system.

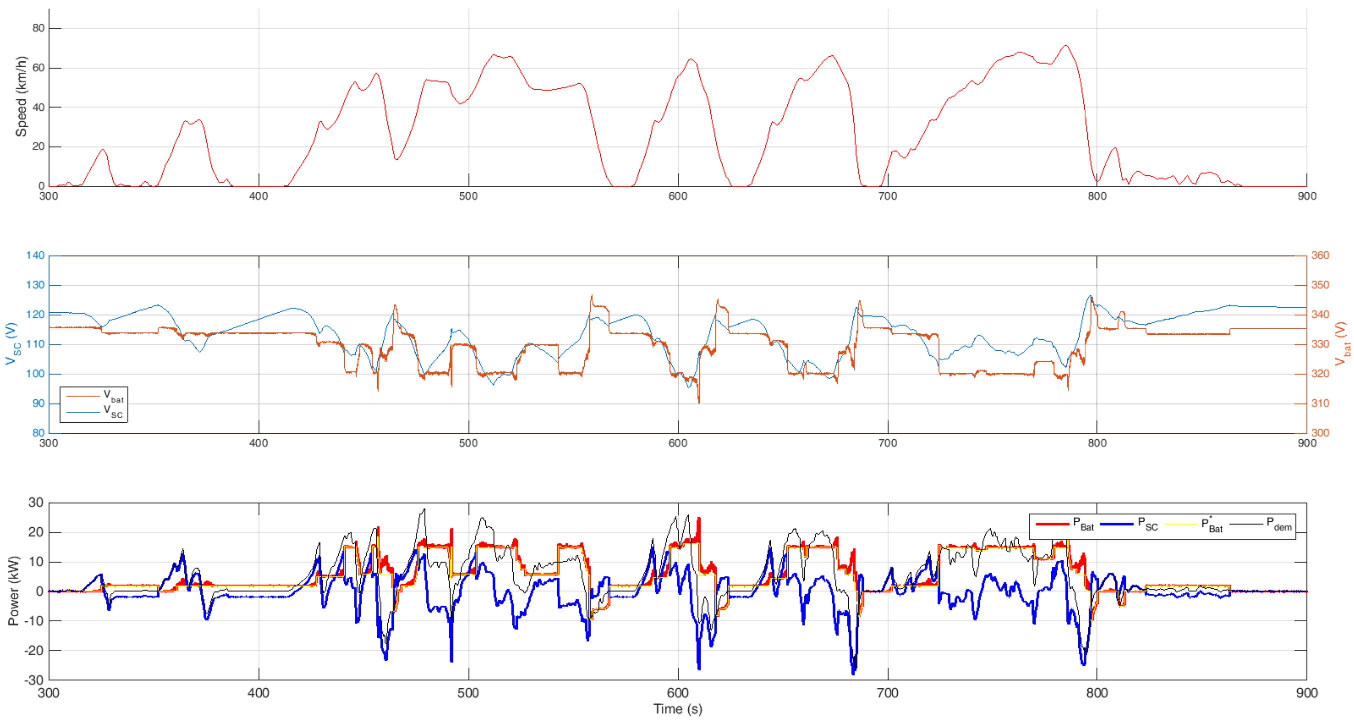

Fig. 8. Simulation results of the e-VUE prototype using a three-level DC-DC converter to couple the SCs pack

ACKNOWLEDGMENT

This work was supported in part by the *Fundação para a Ciência e a Tecnologia* (FCT) under Project Grants UID/MULTI/00308/2013, PTDC/EEA-EEL/121284/2010 and FCOMP-01-0124-FEDER-020391, and also by the National Sciences and Engineering Research Council of Canada.

REFERENCES

[1] Khaligh A., Li Z., "Battery, Ultracapacitor, Fuel Cell, and Hybrid Energy Storage Systems for Electric, Hybrid Electric, Fuel Cell, and Plug-In Hybrid Electric Vehicles: State of the Art", *IEEE Trans. Veh. Tec.*, vol.59, n.6, pp. 2806-2814, Jul. 2010.

[2] Emadi, A.; Rajashekara, K.; Williamson, S.; Lukic, S., "Topological overview of hybrid electric and fuel cell vehicular power system architectures and configurations," *IEEE Trans. Veh. Tec.*, vol.54, no.3, pp.763,770, May 2005

[3] Trovão, J.P.; Pereirinha, P.G., "Control scheme for hybridised electric vehicles with an online power follower management strategy," *Electrical Systems in Transportation, IET*, vol.5, no.1, pp.12-23, 3 2015

[4] Azib T., Bethoux O., Remy G., Marchand C., "Saturation Management of a Controlled Fuel-Cell/Ultracapacitor Hybrid Vehicle", *IEEE Trans. Veh. Tec.*, Vol. 60, n. 9, pp. 4127-4138, Nov. 2011.

[5] Cao J., Emadi A., "A New Battery/UltraCapacitor Hybrid Energy Storage System for Electric, Hybrid, and Plug-In Hybrid Electric Vehicles", *IEEE Trans. Power Electr.*, vol. 27, n. 1, pp. 122-132 Jan. 2012.

[6] Prasanna U., Rathore A., "Extended range ZVS active-clamped current-fed full-bridge isolated DC/DC converter for fuel cell applications: Analysis, design, experimental results," *IEEE Trans. Ind. Electron.*, vol. 60, no. 7, pp. 2661–2672, Jul. 2013.

[7] Xuewei P., Rathore A., "Novel Bidirectional Snubberless Naturally Commutated Soft-Switching Current-Fed Full-Bridge Isolated DC/DC Converter for Fuel Cell Vehicles," *IEEE Trans. Ind. Electron.*, vol. 61, no. 5, pp. 2307–2315, May 2014.

[8] Khaligh A., Emadi, "Mixed DCM/CCM pulse adjustment with constant power loads," *IEEE Trans. Aerosp. Electron. Syst.*, vol. 44, no. 2, pp. 766–782, Apr. 2008.

[9] Rathore A., "Interleaved soft-switched active-clamped L-L type current-fed half-bridge dc–dc converter," *Int. J. Hydrogen Energy*, vol. 34, no. 24, pp. 9802–9815, Dec. 2009.

[10] Rathore A., Prasanna U., "Analysis, Design, Experimental Results of Novel Snubberless Bi-Directional Naturally Clamped ZCS/ZVS Current-Fed Half-Bridge DC/DC Converter For Fuel Cell Vehicles," *IEEE Trans Ind. Electron.*, vol. 60, no. 10, pp. 4482–4491, Oct. 2013.

[11] Grbovic P., Delarue P., Moigne P., Bartholomeus P., "A Bidirectional Three-Level DC–DC Converter for The Ultracapacitor Applications," *IEEE Trans. Ind. Electron.*, vol. 57, no. 10, pp. 3415–3430, Oct. 2010.

[12] Shahin A. et al., "High Voltage Ratio DC–DC Converter for Fuel-Cell Applications," *IEEE Trans. Ind. Electron.*, vol. 57, no. 12, pp. 3944–3954, Dec. 2011.

[13] Po-Wa L., Lee Y., Cheng D., Xiu-Cheng L., "Steady-State Analysis of an Interleaved Boost Converter with Coupled Inductors," *IEEE Trans. Ind. Electron.*, vol. 47, no. 4, pp. 787–795, Aug. 2000.

[14] Machado, F.; Trovao, J.; Antunes, C., "Effectiveness of Supercapacitors in Pure Electric Vehicle Using a Hybrid Meta-Heuristic Approach," *IEEE Trans. Veh. Tec.*, vol. PP, no.99, pp.1,1.

[15] F. R. Salmasi, "Control Strategies for Hybrid Electric Vehicles: Evolution, Classification, Comparison, and Future Trends," *IEEE Transactions on Vehicular Technology*, vol. 56, no. 5, pp. 2393-2404, 2007.

[16] Trovão J., Pereirinha P, Jorge H., Antunes C., "A Multilevel Energy Management System for Multi-Source Electric Vehicles—An Integrated Rule-Based Meta-Heuristic Approach," *Appl. Energy*, vol. 105, pp. 304–318, May 2013.

[17] Trovão J., Antunes C., "A Comparative Analysis Of Meta-Heuristic Methods for Power Management of a Dual Energy Storage System for Electric Vehicles", *Energy Conversion and Management*, vol. 95, pp 281-296, May 2015.